NIH Public Access
Author Manuscript
Science. Author manuscript; available in PMC 2009 September 28.

Published in final edited form as:
Science. 2008 October 17; 322(5900): 405–410. doi:10.1126/science.1162609.

Conservation and Rewiring of Functional Modules Revealed by an Epistasis Map in Fission Yeast

Assen Roguev[1,2], **Sourav Bandyopadhyay**[3], **Martin Zofall**[4], **Ke Zhang**[4], **Tamas Fischer**[4], **Sean R. Collins**[1,2,5], **Hongjing Qu**[1,2], **Michael Shales**[1,2], **Han-Oh Park**[6], **Jacqueline Hayles**[7], **Kwang-Lae Hoe**[8], **Dong-Uk Kim**[8], **Trey Ideker**[3,*], **Shiv I. Grewal**[4,*], **Jonathan S. Weissman**[1,2,5,*], and **Nevan J. Krogan**[1,2,*]

[1]Department of Cellular and Molecular Pharmacology, University of California, San Francisco, CA 94158, USA

[2]California Institute for Quantitative Biosciences, University of California, San Francisco, CA 94158, USA

[3]Department of Bioengineering and Program in Bioinformatics, University of California-San Diego, La Jolla, CA 92093, USA

[4]Laboratory of Biochemistry and Molecular Biology, Center for Cancer Research, National Cancer Institute, NIH, Bethesda, MD 20892, USA

[5]Howard Hughes Medical Institute, San Francisco, CA 94158, USA

[6]Bioneer Corporation, Daejeon, Korea

[7]Cell Cycle Laboratory, Cancer Research UK, London Research Institute, 44 Lincoln's Inn Fields, London WC2A 3PX, UK

[8]Genomic Research Center, Korea Research Institute of Bioscience and Biotechnology, Daejeon, Korea

Abstract

An epistasis map (E-MAP) was constructed in the fission yeast, *Schizosaccharomyces pombe*, by systematically measuring the phenotypes associated with pairs of mutations. This high-density, quantitative genetic interaction map focused on various aspects of chromosome function, including transcription regulation and DNA repair/replication. The E-MAP uncovered a previously unidentified component of the RNA interference (RNAi) machinery (*rsh1*) and linked the RNAi pathway to several other biological processes. Comparison of the *S. pombe* E-MAP to an analogous genetic map from the budding yeast revealed that, whereas negative interactions were conserved between genes involved in similar biological processes, positive interactions and overall genetic profiles between pairs of genes coding for physically associated proteins were even more conserved. Hence, conservation occurs at the level of the functional module (protein complex), but the genetic cross talk between modules can differ substantially.

Genetic interactions report on the extent to which the function of one gene depends on the presence of a second. This phenomenon, known as epistasis, can be used for defining functional relationships between genes and the pathways in which the corresponding proteins function.

*To whom correspondence should be addressed. E-mail: trey@bioeng.ucsd.edu (T.I.); grewals@mail.nih.gov (S.I.G.); weissman@cmp.ucsf.edu (J.S.W.); krogan@cmpmail.ucsf.edu (N.J.K.).

Supporting Online Material www.sciencemag.org/cgi/content/full/1162609/DC1 Materials and Methods SOM Text Figs. S1 to S5 Tables S1 to S8 References Databases S1 to S4

NIH-PA Author Manuscript
NIH-PA Author Manuscript
NIH-PA Author Manuscript

NIH-PA Author Manuscript

NIH-PA Author Manuscript

NIH-PA Author Manuscript

Two main categories of genetic interactions exist: (i) negative (e.g., synthetic sickness/lethality) and (ii) positive (e.g., suppression). We have developed a quantitative approach, termed epistasis map (E-MAP), allowing us to measure the whole spectrum of genetic interactions, both positive and negative (1,2). In budding yeast, *Saccharomyces cerevisiae*, it has been demonstrated that positive genetic interactions can identify pairs of genes whose products are physically associated and/or function in the same pathway (1,2), whereas negative interactions exist between genes acting on parallel pathways (3,4).

We developed the Pombe Epistasis Mapper (PEM) approach (5) that allows high-throughput generation of double mutants in the fission yeast, *Schizosaccharomyces pombe*. Fission yeast is more similar to metazoans than is *S. cerevisiae*, owing to its large complex centromere structure, the restriction of spindle construction to mitotic entry, gene regulation by histone methylation and chromodomain heterochromatin proteins, gene and transposon regulation by the RNA interference (RNAi) pathway, and the widespread presence of introns in genes. To further study these processes and to try to understand how genetic interaction networks have evolved (6), we generated an E-MAP in *S. pombe* that focuses on nuclear function, designed to be analogous to one we created in budding yeast (2).

An E-MAP in *S. pombe*

Using our PEM system (5), we generated a quantitative genetic interaction map in *S. pombe*, comprising ~118,000 distinct double mutant combinations among 550 genes involved in various aspects of chromosome function (Fig. 1A and tables S1 and S4) (7). The genes on the map were chosen on the basis of a previous budding yeast E-MAP (1,2) and also included factors present in human (but not in *S. cerevisiae*), including the RNAi machinery. We used colony size (measured from high-density arrays) as a quantitative phenotypic read-out to compute a genetic interaction score (S score) and previously described quality control measures to ensure a high-quality data set (7,8) (fig. S1A).

We have previously observed two prominent general trends between genetic interactions and protein-protein interactions (PPIs): (i) a propensity for positive genetic interactions and (ii) strong correlations of genetic interaction profiles between genes coding for proteins participating in PPIs (2). Using a high-confidence set of 151 PPI pairs from *S. pombe* (9) (table S2), we observed the same trends in this organism (Fig. 1, B and C). Thus, it appears these relationships are evolutionarily conserved and may represent a general feature of biological networks.

Exploring nuclear function in fission yeast

We generated a highly structured representation of the genetic map by subjecting the data to hierarchical clustering (Fig. 2). By scrutinizing several interaction-rich regions, we were able to recapitulate known, and identify previously unknown, functional relationships.

Genes required for DNA repair/recombination and various checkpoint functions form clusters enriched in negative interactions (Fig. 2, region 1). The *rad9-hus1-rad1* (9-1-1) checkpoint complex (10) clusters together with rad17 (the homolog of budding yeast *RAD24*), which loads it onto DNA (11). We found two genes linked to tRNA bio-genesis, *sen1* and *trm10*, within the DNA repair cluster. tRNA regulation has been linked to the DNA damage response pathway in *S. cerevisiae* (12), and these genetic patterns suggest that a similar mechanism may exist in fission yeast. To genetically interrogate the function of essential genes, we used the decreased abundance by mRNA perturbation (DAmP) strategy for generating hypomorphic alleles (1) (table S1) and found that the DAmP allele of *mcl1*, involved in DNA replication control and repair, is highly correlated with components of the replication checkpoint (*mrc1* and *csm3*).

NIH-PA Author Manuscript

NIH-PA Author Manuscript

NIH-PA Author Manuscript

The fission yeast homologs of the components of the SWR complex (SWR-C)—which, in budding yeast, incorporates the histone H2A variant Htz1 (Pht1 in fission yeast) into chromatin (13-15)—form a highly correlated group (Fig. 2, region 2). A jumonji domain-containing protein, Msc1, whose *S. cerevisiae* ortholog *ECM5* is not part of the budding yeast's SWR-C, is found within the fission yeast SWR-C cluster, consistent with the demonstration that Msc1 acts through Pht1 to promote chromosome stability (16).

The E-MAP reveals functional specialization of the fission yeast Set1 histone H3 lysine 4 methyltransferase complex (SET1-C, COMPASS) (17-20). In *S. pombe*, five of its subunits (core SET1-C: *set1*, *spp1*, *swd1*, *swd21*, and *swd3*) are indispensable for H3-K4 methylation (19) and form a highly correlated cluster on the E-MAP (Fig. 2, region 3). In budding yeast, another component of COMPASS, Swd2, is essential and is part of two distinct complexes: (i) SET1-C and the (ii) Cleavage and Polyadenylation Factor (CPF) (17,21). *S. pombe* contains two nonessential paralogs of *SWD2* (*swd21* and *swd22*), which have previously been shown to act independently in the *S. pombe* SET1-C and CPF, respectively (22). Consistent with this observation, on our map, *swd21* is part of the core SET1-C, whereas *swd22* is strongly correlated with the *SSU72* ortholog, a part of CPF (21,23) (Fig. 2, region 3). The Ash2-Sdc1 heterodimer within the SET1-C also behaves differently. In *S. cerevisiae*, its orthologous pair (Bre2p-Sdc1p) is exclusively found in the SET1-C (17), whereas in fission yeast it is shared between the SET1-C and LID2-C (19). Consistent with this result, the dimer does not cluster next to core Set1-C [as is observed in budding yeast (2)] but is more similar to *snt2*, a member of LID2-C (Fig. 2, region 3).

Genetic dissection of the RNAi pathway

The RNAi pathway in *S. pombe* is composed of several components, including CLR4-C, RDR-C, RITS, dicer (Dcr1), and the HP1 homolog Swi6 (24). All known components of the RNAi machinery that were analyzed cluster next to each other and primarily display positive genetic interaction with one another (Fig. 3A). Within this cluster are subclusters corresponding to the different protein complexes. Consistent with previous reports, we found positive genetic interactions between the RNAi machinery and *epe1*, an anti-silencing factor involved in the transcription of heterochromatic regions by RNA polymerase II (RNAPII) (25) and required for RNAi-mediated heterochromatin assembly (24). Conversely, we found negative interactions between RNAi components involved in posttranscriptional gene silencing and factors implicated in transcriptional gene silencing (TGS) of repeat sequences and other loci. In particular, *clr3*, a histone deacetylase and catalytic subunit of the Snf2/Hdac-containing repressor complex (26) that is involved in TGS at centromeric repeats (24) and Tf2 retrotransposons (27,28), shows negative interactions with RNAi components (Fig. 3A).

Within the RNAi cluster, we also found a previously unknown component of the RNAi pathway, SPCC1393.05, which we named *rsh1* (involved in RNAi silencing and heterochromatin formation) (Fig. 3A). The gene encodes a 110-kD protein with no obvious homologs or apparent sequence motifs. We used chromatin immunoprecipitation to determine that Rsh1 is localized to heterochromatic centromeric regions. Its absence causes a substantial reduction of silencing at these loci and a loss of small interfering RNAs (siRNAs) expressed from the centromeric dg/dh repeats (Fig. 3, B to F). Additionally, *rsh1*Δ leads to a marked reduction of H3-K9 dimethylation and Swi6/HP1 binding that correlates with lowered levels (more than sixfold decrease) of Ago1 (a component of RITS) recruitment to the outer (*otr*) centromeric repeat region (Fig. 3, G and H).

We also observed positive interactions between the RNAi machinery and homologs of factors involved in the transition between transcriptional initiation and elongation, including *rpb9* and *iwr1*, components of RNAPII (21,29), and the Mediator complex (*pmc2*, *rox3*, *pmc5*,and

NIH-PA Author Manuscript

NIH-PA Author Manuscript

NIH-PA Author Manuscript

med2)(30,31). Deletions of *rpb9, rox3, pmc5*,or *pmc2* lead to moderate loss of silencing at the centromere (Fig. 3, I and J).

We observed numerous negative genetic interactions between the RNAi machinery and other cellular complexes and processes (Fig. 3A), including the spindle-checkpoint pathway (*mad1, mad2, bub3*,and *alp14*)(32); components of the DASH complex (33) (*dad1, dad2, ask1*, and *spc34*); and *mal3, tub1, and alp31* involved in microtubule stability (34), consistent with the involvement of RNAi/heterochromatin apparatus in proper chromosome segregation (35). The acetyltrasferase complex Elongator (36) interacts negatively with the RNAi machinery and clusters next to factors regulating spindle function, consistent with the observation that Elongator may be responsible for tubulin acetylation, required for microtubule-based protein trafficking (37). Finally, components of the DNA repair, checkpoint, and recombination apparatus display negative genetic interactions with the RNAi machinery, suggesting that the RNAi pathway is also involved in maintaining genomic stability.

Conservation of modular organization of genetic interaction networks

The large evolutionary distance between *S. cerevisiae* and *S. pombe* [~400 million years (38)] allowed us to study the evolution of genetic interactomes. We directly compared the data from this *S. pombe* E-MAP to an analogous database from *S. cerevisiae* (database S4) (2). The overlap of one-to-one annotated orthologs (39) between the two E-MAPs encompasses 239 genes (table S3). First, we analyzed individual negative pairwise interactions in the two organisms. Recently, it has been suggested (6) that negative interactions between yeast and *Caenorhabditis elegans* were not conserved. Although not strong, we did find a conservation of negative interactions (17.3% for S score $\leq$ -2.5), which became more pronounced (33%) when the analysis was restricted to genes that shared the same functional annotations (Fig. 4A and fig. S2B). To confirm this observation, we used an independent data set from BioGRID (9) and observed similar conservation rates [18% for all and 31% among functionally related genes (7)]. Part of the discrepancy seen in *C. elegans* could be due to functional redundancy, multicellularity, or incomplete knockdowns by RNAi. Furthermore, this comparison was not restricted to functionally related genes (6). In our analysis, we also found a very strong conservation (>50%) of positive interactions (S score $\geq$ 2.0) [that were not considered by (6)] between pairs of genes whose corresponding proteins are physically associated (Fig. 4A and fig. S2, A to D) (7).

The set of genetic interactions for a given gene provides a sensitive phenotypic signature or profile. Although a global comparison of all correlations of genetic profiles between orthologous pairs in each species (table S3) revealed a weak overall conservation (correlation coefficient $r = 0.14$) (Fig. 4B), pairs corresponding to PPIs were much more highly correlated ($r = 0.60$) (Fig. 4B). An aggregate measure for the likelihood of two proteins to carry out a common function, many of which correspond to PPI pairs, is the complex or linear pathway (COP) score (8), which integrates the individual genetic interaction score and correlation coefficient of genetic interaction profiles. Pairs of genes displaying high COP scores in both organisms almost exclusively correspond to PPIs (fig. S2E).

To further explore the extent of conservation of genetic networks, the profiles of each of the 239 orthologs in both species were compared to all profiles from the other organism (Fig. 4C). We found some conservation between direct orthologs ($P = 8 \times 10^{-20}$), suggesting that genetic interaction profiles of orthologs across species tend to be similar (fig. S2F). There is, however, a stronger conservation of genetic profiles between a gene and the ortholog of its interacting partner when only co-complex members were considered (Fig. 4C) ($P = 9 \times 10^{-51}$). Thus, genetic profiles of members of PPI pairs tend to correlate better, not only to their interaction

NIH-PA Author Manuscript

NIH-PA Author Manuscript

NIH-PA Author Manuscript

partners within the same species, but also to the orthologs of their interaction partner in an evolutionarily distant organism.

Collectively, these data demonstrate that genetic interactions between particular subsets of genes are conserved between *S. cerevisiae* and *S. pombe*. Specifically, we find conservation of negative interactions when genes involved in the same cellular process are considered. Better conserved are positive interactions and genetic profiles of genes whose products are physically associated. Therefore, we argue that conservation primarily exists at the level of the functional module (protein complex), and perhaps PPIs pose a constraint on functional divergence in evolution.

Rewiring of conserved functional modules

Biological modules can be defined as highly interconnected groups of physically or functionally associated factors, and they often correspond to protein complexes. In addition to identifying functional modules, high-density genetic interaction data reports on the functional relationships between modules (i.e., the wiring of the network).

To compare the genetic cross talk between modules in the two organisms, we merged and clustered the genetic interaction matrix of *S. pombe* with that of *S. cerevisiae* for the 239 1:1 orthologs (database S2). Inspection of this database revealed a partial overlap of negative interactions between protein complexes (Fig. 5A). For example, in both organisms, SWR-C display negative genetic interactions with the SET1-C and the histone deacetylatase (HDAC) complex, SET3-C. However, substantial differences were found as well. For instance, only in budding yeast are there negative interactions between SWR-C and components of the spindle checkpoint, the chaperone complex Prefoldin, the HDAC complex, Rpd3C(L), and Mediator (Fig. 5A).

Several possible explanations can be offered. First, the additional subunit unique to the fission yeast SWR-C, Msc1, may alter the function of the complex. Also, species-specific posttranslational modifications may result in different genetic behavior. Msc1 has been shown to harbor ubiquitin ligase activity (40)and may be involved in ubiquitinating proteins related to the function of SWR-C. Another reason could be the presence or absence of particular cellular machinery. For example, the rewiring of the genetic space surrounding the SWR-C in *S. pombe* may be due to the presence of the RNAi machinery, which shows negative interactions with the complex (Fig. 5B). Consequently, dramatic alterations in the network topology of budding yeast may have been necessary to compensate for the absence of the RNAi pathway. We cannot rule out the possibility that many of the interactions do exist under different environmental conditions. Nonetheless, a major rewiring of other complexes [e.g., the histone regulatory (HIR) chromatin assembly complex and Prefoldin] (fig. S3) was also observed under the conditions used.

The modularity of biological networks is believed to be one of the main contributors to their robustness, as it implies enhanced functional flexibility. Much like an electronic circuit, such modular architecture allows different tasks to be accomplished with the same minimal set of components by changing the wiring (or flow of information) between them. Rewiring because of addition or removal of modules allows for economical design of sophisticated networks that are able to adapt to different conditions and environmental niches at a low cost. We observe this behavior derived from high-density genetic-interaction data from two evolutionarily distant species. Our data strongly support the idea that functional modules are highly conserved, but the wiring between them can differ substantially. Thus, the use of model systems to make inferences about biological network topology may be more successful for describing modules than for describing the cross talk between them.

NIH-PA Author Manuscript

NIH-PA Author Manuscript

NIH-PA Author Manuscript

Supplementary Material

Refer to Web version on PubMed Central for supplementary material.

Acknowledgments

We thank P. Beltrao and G. Cagney for critical reading of the manuscript; M. Wiren and S. Forsburg for discussion; P. Kemmeren for setting up the web database; S. Wang, C. Wen, and D. Avdic for technical help; and F. Stewart for sharing unpublished data. This work was supported by NIH [National Institute of General Medical Sciences grant GM084279 (T.I. and N. J.K.)], the Sandler Family Foundation (N.J.K), the Howard Hughes Medical Institute (J.S.W.), National Cancer Institute (S.I.G.), Center for Cancer Research (S.I.G.), and the California Institute of Quantitative Biology (N.J.K.)

References and Notes

1. Schuldiner M, et al. Cell 2005;123:507. [PubMed: 16269340]
2. Collins SR, et al. Nature 2007;446:806. [PubMed: 17314980]
3. Pan X, et al. Methods 2007;41:206. [PubMed: 17189863]
4. Tong AHY, et al. Science 2004;303:808. [PubMed: 14764870]
5. Roguev A, Wiren M, Weissman JS, Krogan NJ. Nat. Methods 2007;4:861. [PubMed: 17893680]
6. Tischler J, Lehner B, Fraser AG. Nat. Genet 2008;40:390. [PubMed: 18362882]
7. Materials and methods are available as supporting material on *Science* Online
8. Collins SR, Schuldiner M, Krogan NJ, Weissman JS. Genome Biol 2006;7:R63. [PubMed: 16859555]
9. Stark C. Nucleic Acids Res 2006;34:D535. [PubMed: 16381927]
10. Kaur R, Kostrub CF, Enoch T. Mol. Biol. Cell 2001;12:3744. [PubMed: 11739777]
11. Majka J, Burgers PM. Proc. Natl. Acad. Sci. U.S.A 2003;100:2249. [PubMed: 12604797]
12. Ghavidel A, et al. Cell 2007;131:915. [PubMed: 18045534]
13. Krogan NJ, et al. Mol. Cell 2003;12:1565. [PubMed: 14690608]
14. Mizuguchi G, et al. Science 2004;303:343. [PubMed: 14645854]published 26 November 2003; 10.1126/science.1090701
15. Kobor MS, et al. PLoS Biol 2004;2:E131. [PubMed: 15045029]
16. Ahmed S, Dul B, Qiu X, Walworth NC. Genetics 2007;177:1487. [PubMed: 17947424]
17. Roguev A, et al. EMBO J 2001;20:7137. [PubMed: 11742990]
18. Krogan NJ, et al. J. Biol. Chem 2002;277:10753. [PubMed: 11805083]
19. Roguev A, et al. J. Biol. Chem 2003;278:8487. [PubMed: 12488447]
20. Nagy PL, Griesenbeck J, Kornberg RD, Cleary ML. Proc. Natl. Acad. Sci. U.S.A 2002;99:90. [PubMed: 11752412]
21. Gavin AC, et al. Nature 2002;415:141. [PubMed: 11805826]
22. Roguev A, et al. Mol. Cell. Proteomics 2004;3:125. [PubMed: 14617822]
23. Dichtl B, et al. Mol. Cell 2002;10:1139. [PubMed: 12453421]
24. Grewal SI, Jia S. Nat. Rev. Genet 2007;8:35. [PubMed: 17173056]
25. Zofall M, Grewal SI. Mol. Cell 2006;22:681. [PubMed: 16762840]
26. Sugiyama T, et al. Cell 2007;128:491. [PubMed: 17289569]
27. Hansen KR, et al. Mol. Cell. Biol 2005;25:590. [PubMed: 15632061]
28. Cam HP, Noma K, Ebina H, Levin HL, Grewal SI. Nature 2008;451:431. [PubMed: 18094683]
29. Krogan NJ. Nature 2006;440:637. [PubMed: 16554755]
30. Spahr H. J. Biol. Chem 2000;275:1351. [PubMed: 10625684]
31. Sakurai H, Kimura M, Ishihama A. Gene 1998;221:11. [PubMed: 9852944]
32. Millband DN, Hardwick KG. Mol. Cell. Biol 2002;22:2728. [PubMed: 11909965]
33. Liu X, McLeod I, Anderson S, Yates JR III, He X. EMBO J 2005;24:2919. [PubMed: 16079914]
34. Asakawa K. Mol. Biol. Cell 2006;17:1421. [PubMed: 16394105]
35. Hall IM, Noma K, Grewal SI. Proc. Natl. Acad. Sci. U.S.A 2003;100:193. [PubMed: 12509501]

NIH-PA Author Manuscript

NIH-PA Author Manuscript

NIH-PA Author Manuscript

36. Otero G, et al. Mol. Cell 1999;3:109. [PubMed: 10024884]
37. Gardiner J, Barton D, Marc J, Overall R. Traffic 2007;8:1145. [PubMed: 17605759]
38. Sipiczki M. Genome Biol 2000;1REVIEWS1011
39. Penkett CJ, Morris JA, Wood V, Bahler J. Nucleic Acids Res 2006;34:W330. [PubMed: 16845020]
40. Dul BE, Walworth NC. J. Biol. Chem 2007;282:18397. [PubMed: 17456468]
41. Bandyopadhyay S, Kelley R, Krogan NJ, Ideker T. PLOS Comput. Biol 2008;4:e1000065. [PubMed: 18421374]

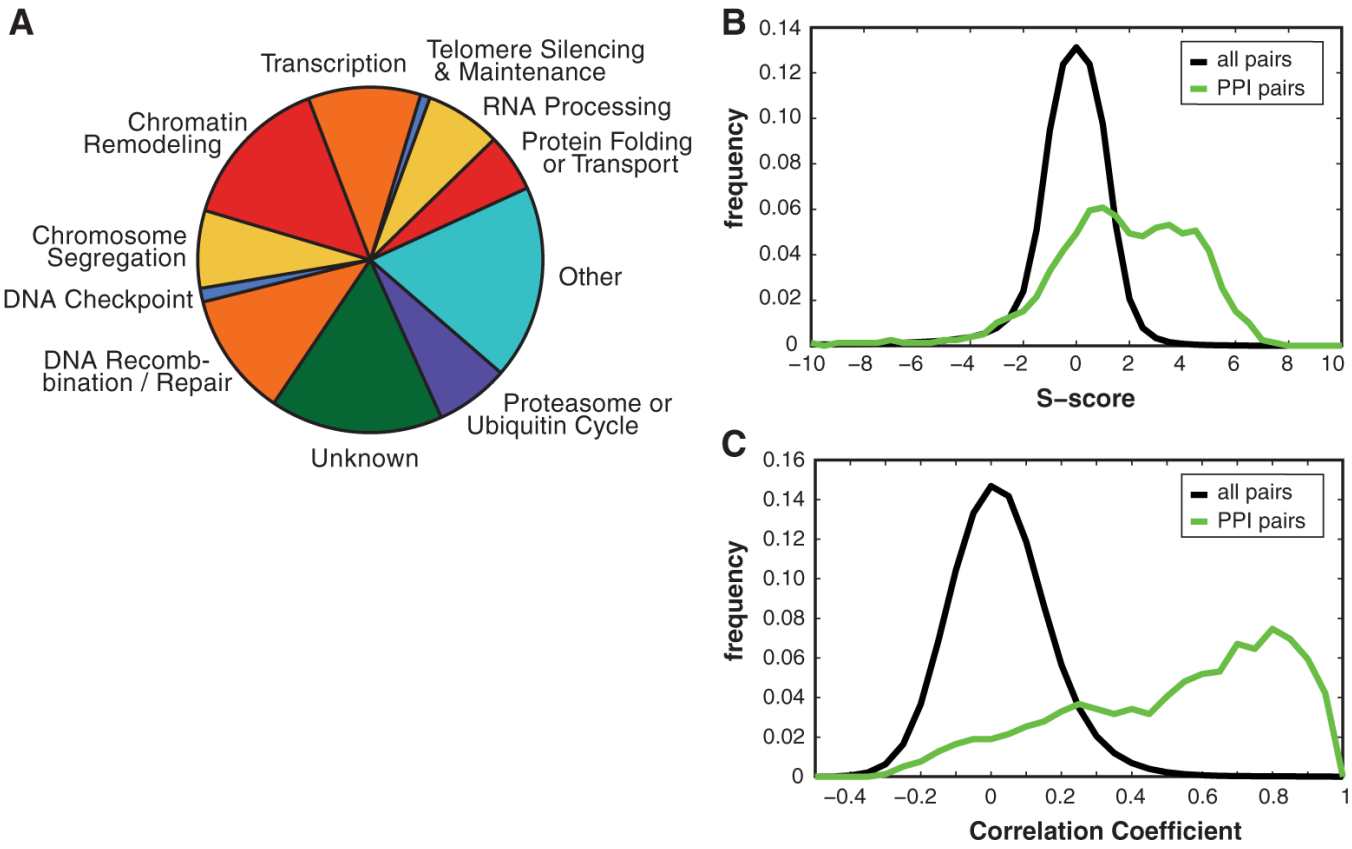

Fig. 1.

Data set overview. (**A**) Functional classification of the genes contained within the *S. pombe* E-MAP. The map contains 550 genes that were classified into 11 functional categories (table S4). (**B**) Distribution of interaction scores for pairs of genes corresponding to physically interacting proteins (green) and noninteracting proteins (black). (**C**) Distribution of Pearson correlation coefficients of the genetic interaction profiles for the same set of genes used in (B). For a complete list of PPIs used in this analysis, see table S2.

NIH-PA Author Manuscript NIH-PA Author Manuscript NIH-PA Author Manuscript

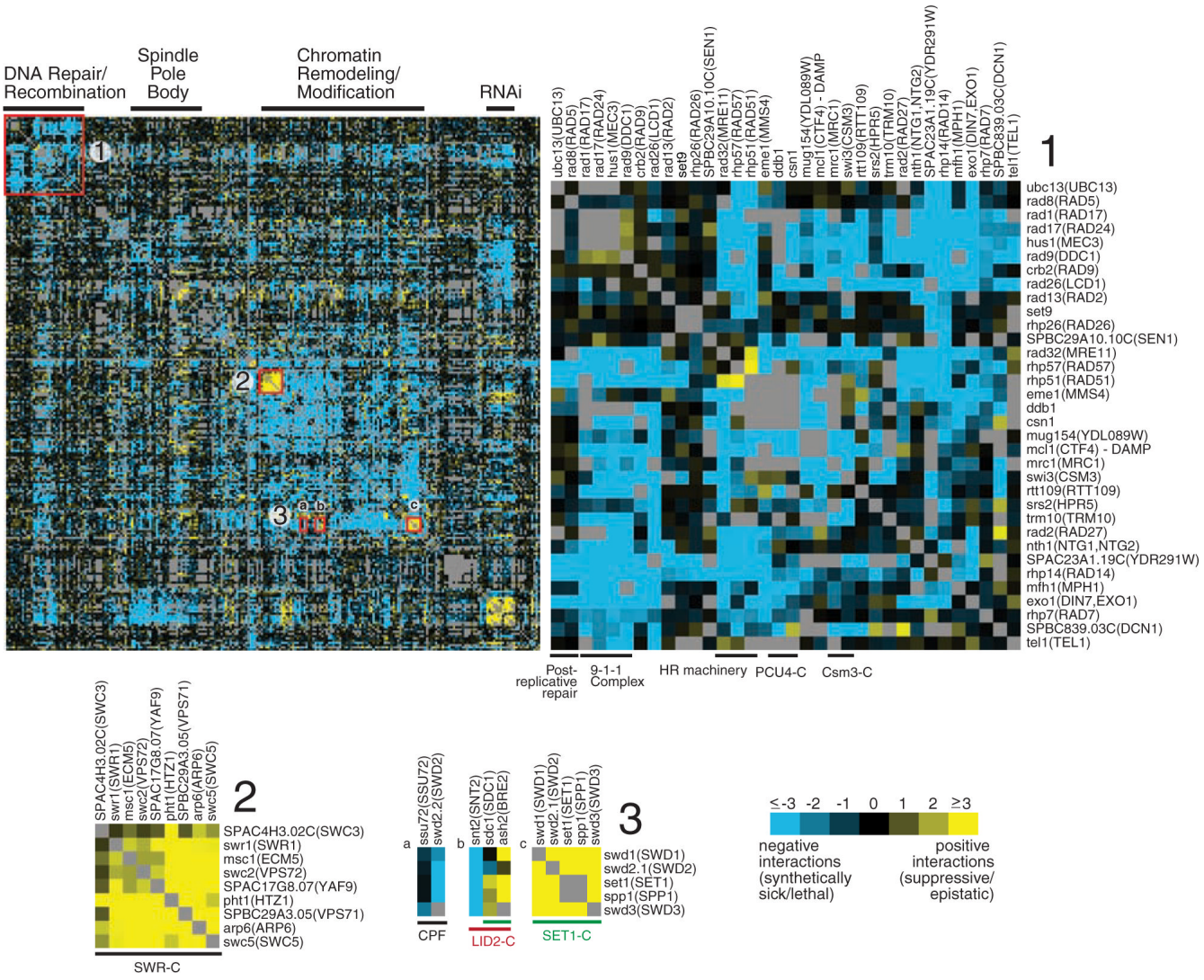

Fig. 2.

The *S. pombe* chromosome function E-MAP. A section of the E-MAP with specific regions of interest annotated. Further highlighted are the factors involved in DNA repair/recombination (1), as well as two complexes contained within the chromatin remodeling/modification region: the SWR-C chromatin remodeling complex (2) and the Set1, Lid2, and CPF complexes (3). The names of the budding yeast orthologs are shown in parentheses (table S3). The final data set consists of 118,575 measurements and contains 5772 negative (S score ≤ -2.5) and 1812 positive (S score ≥ 2) interactions.

NIH-PA Author Manuscript
NIH-PA Author Manuscript
NIH-PA Author Manuscript

NIH-PA Author Manuscript
NIH-PA Author Manuscript
NIH-PA Author Manuscript

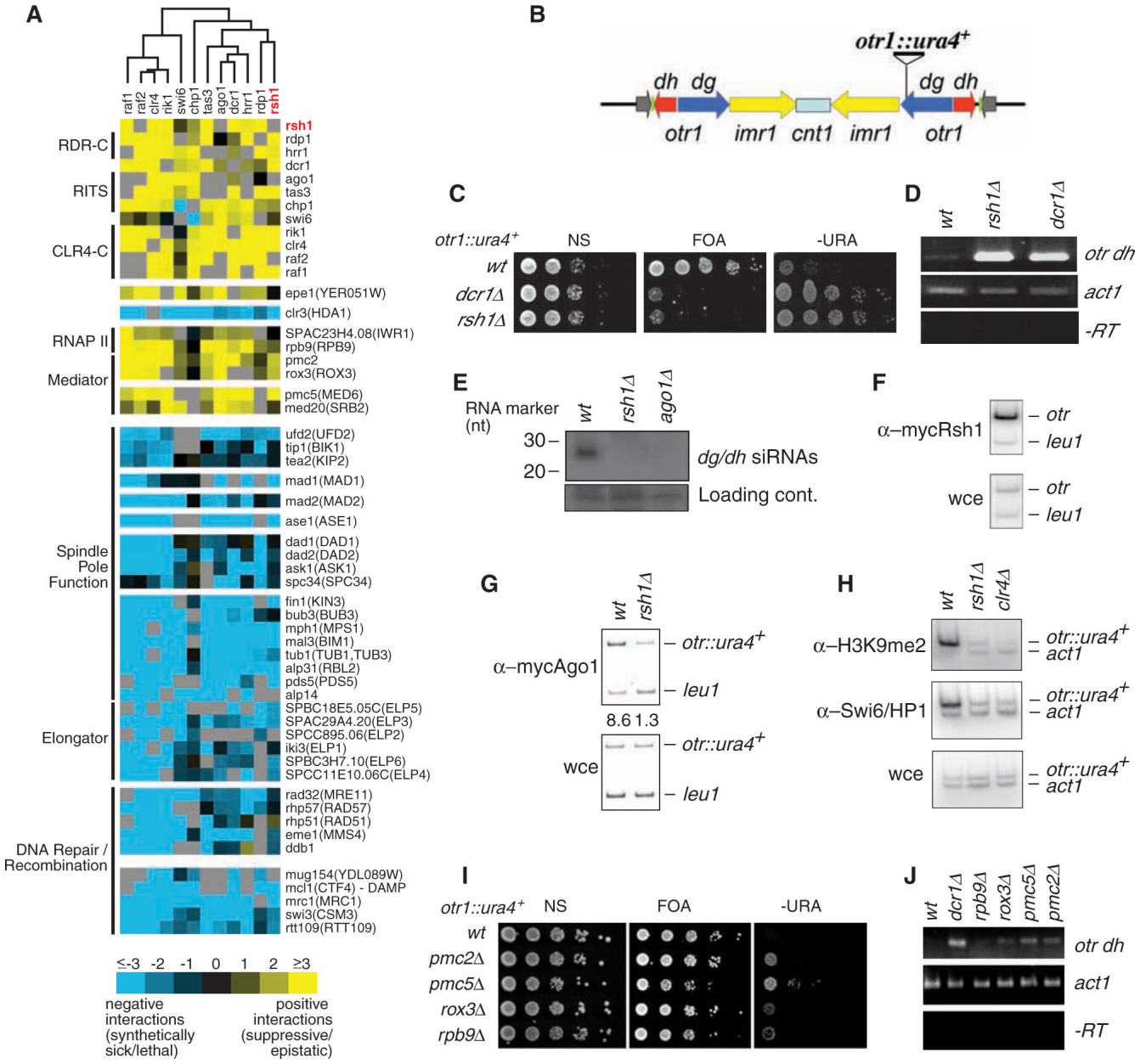

Fig. 3.

Characterization of genes involved in the RNAi pathway. (**A**) Genetic profiles for genes involved in RNAi with individual protein complexes or processes annotated. (**B**) Schematic of the centromeric region of chromosome 1 with the position of the *ura4*$^+$ reporter gene within the *otr1* region. (**C**) Loss of Rsh1p abolishes heterochromatic silencing of the *ura4*$^+$ reporter gene inserted at the outer repeat region of centromere 1 (*otr1*::*ura4*$^+$). NS, nonselective; FOA, counterselective; -URA, uracil-deficient media. (**D**) Levels of *dh* transcripts analyzed by reverse transcription polymerase chain reaction (RT-PCR) using RNA prepared from indicated strains. (*E*) Loss of siRNAs derived from *dg/dh* repeats in *rsh1*Δ detected by Northern blotting. nt, nucleotides. (**F**)Rsh1 localizes to outer (*otr*) centromeric repeats. An epitope-tagged version of Rsh1 (mycRsh1) was used to perform chromatin immunoprecipitation (ChIP). wce, whole-cell extract. (**G**) Rsh1 is required for localization of Ago1. Localization of mycAgo1 at *otr1*::*ura4*$^+$ in wild-type and *rsh1*Δ cells was assayed using ChIP. leu1 is an internal loading

NIH-PA Author Manuscript

NIH-PA Author Manuscript

NIH-PA Author Manuscript

control for ChIP experiments. (*H*) Effect of *rsh1*Δ on heterochromatin assembly at centromeric repeats. Levels of histone H3 lysine 9 dimethylation (H3K9me2) and Swi6/HP1 at *otr1*::*ura4*$^{+}$ were assayed using ChIPs. (**I** and **J**) Loss of Mediator and RNAPII subunits affects centromeric silencing. The levels of transcripts corresponding to **dh** centromeric repeats were analyzed by RT-PCR. leu1 and act1 are used as internal loading controls.

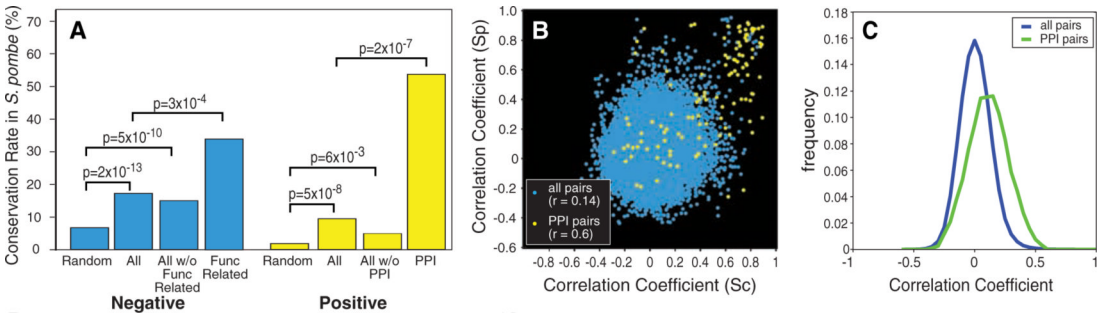

Fig. 4.

Modular conservation of genetic interaction patterns. A set of 239 one-to-one orthologs (table S3) was used for the analysis. (**A**) Conservation of positive and negative genetic interactions based on comparison with *S. cerevisiae*. Conservation rates are higher for the subset of negative interactions between genes with the same functional annotation and the subset of positive interactions corresponding to known PPIs in *S. cerevisiae*. Pairs of genes whose proteins are physically associated or functionally related did not contribute significantly to the general trends (second bar), because removal of these pairs (third bar) resulted in similar conservation rates. *P* values were determined using a two-sided Student's *t* test (7). (**B**) Scatter plot of Pearson correlation coefficients of genetic interaction profiles. Sc, *S. cerevisiae*; Sp, *S. pombe*. (C) Distribution of the cross-species Pearson correlation coefficient of genetic profiles.

NIH-PA Author Manuscript NIH-PA Author Manuscript NIH-PA Author Manuscript

NIH-PA Author Manuscript
NIH-PA Author Manuscript
NIH-PA Author Manuscript

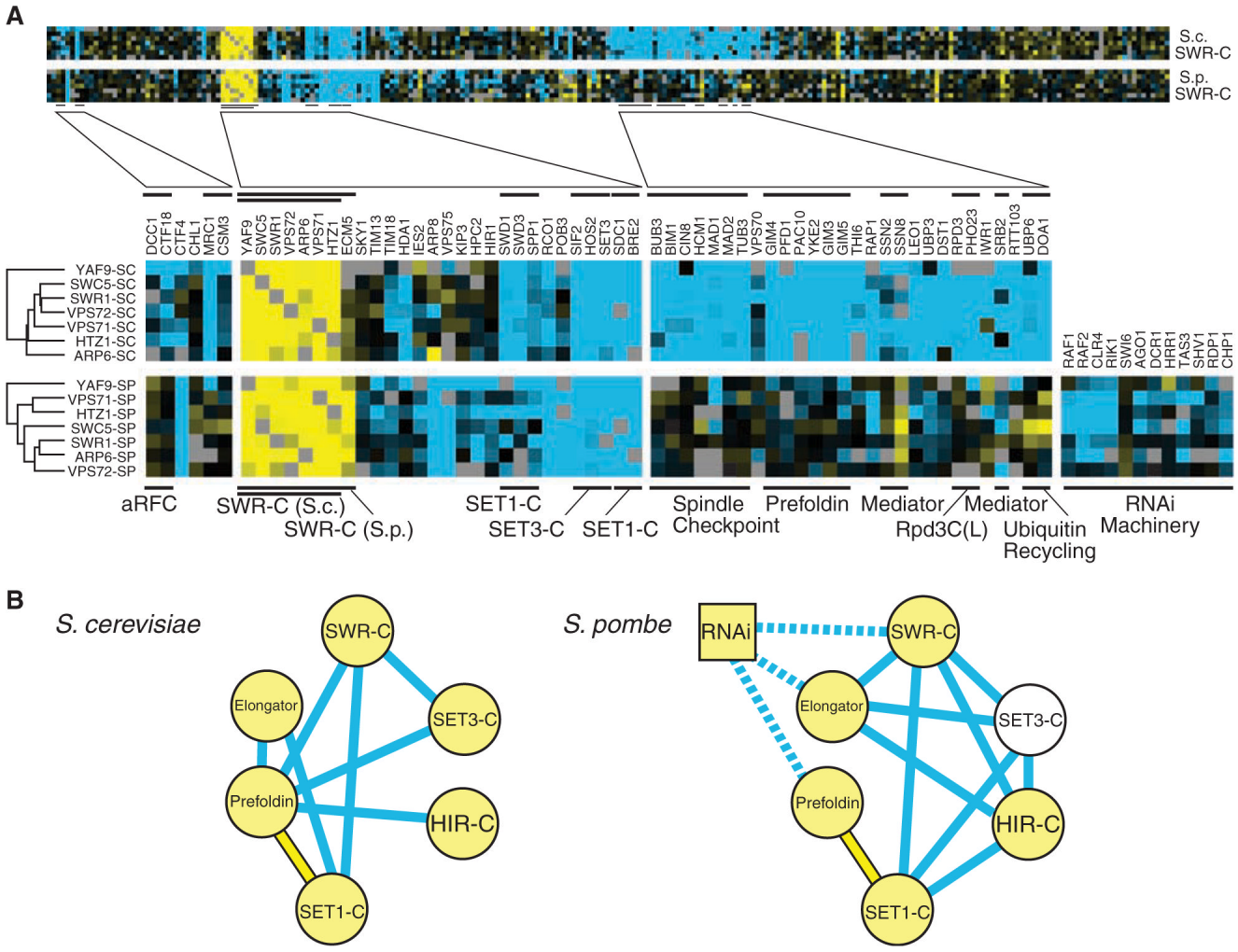

Fig. 5.

Rewiring of the conserved functional modules. (**A**) Comparison of genetic interaction profiles of the SWR-C in *S. cerevisiae* and *S. pombe*. Analogous sets of genetic interactions from the two organisms are shown (database S2). (**B**) Genetic cross talk between functional modules. Modules are represented as circles or boxes (in yellow if the interactions within the module are primarily positive). Negative and positive interactions between modules are represented as blue and yellow lines, respectively. The diagram was generated using the method described in (41).